MAGNETIC RESONANCE IN CHEMISTRY, VOL. 34, S81–S86 (1996)

# NMR Study of the Interaction of the HU Protein from *Bacillus Stearothermophilus* with DNA

**Hans Vis, Olga Vageli and Jord Nagel**
Bijvoet Center for Biomolecular Research, University of Utrecht, Padualaan 8, 3584 CH Utrecht, The Netherlands

**Constantin E. Vorgias and Keith S. Wilson**
European Molecular Biology Laboratory (EMBL), c/o DESY, Notkestrasse 85, D-22603 Hamburg, Germany

**Robert Kaptein* and Rolf Boelens**
Bijvoet Center for Biomolecular Research, University of Utrecht, Padualaan 8, 3584 CH Utrecht, The Netherlands

**DNA binding of the 19.5 kDa protein HU from *Bacillus stearothermophilus* (HUBst) with several non-specific double-stranded DNA oligomers was studied using NMR techniques. Photochemically induced nuclear polarization (photo-CIDNP) measurements on a mutant HUBst (M69Y; V76Y) show that Y69 in the tip of the β-hairpin arm is involved in DNA interaction. Changes in $^{15}N$ and $^{1}H^{N}$ chemical shifts upon titrating DNA are greatest for the residues in the β-hairpin arm and for the residues in the second half of the third α-helix. The changes in the flexible arms can be interpreted as being due to the formation of more rigid secondary structure upon DNA binding. Backbone and side-chain dynamics of HUBst were investigated using heteronuclear $^{15}N$–$^{1}H^{N}$ NOE, $^{15}N$ $T_1$ and $T_{1\rho}$ data for free and complexed HUBst. These measurements show that the mobility of the flexible arms reduces in the protein–DNA complex. The results demonstrate that the β-hairpin arms and the C-terminal α-helix of HUBst are involved in DNA binding.**

KEY WORDS NMR; $^{1}H$ NMR; $^{15}N$ NMR; photo-CIDNP; heteronuclear NOE; relaxation measurements; mutant HU; DNA-binding protein

## INTRODUCTION

The type II DNA-binding proteins (DBP II) are a family of homologous, dimeric and usually basic proteins found abundantly in all prokaryotes.[1,2] The protein HU and other DBP II proteins bind to DNA without obvious sequence specificity. The only members of the DBP II family that exhibit sequence specificity in DNA binding are the integration host factor (IHF)[3–6] and transcription factor I (TF1) encoded by bacteriophage SPO1.[7,8] It has been demonstrated recently that HU can functionally replace IHF in site-specific recombination assays.[9] DBP II proteins have the ability to bend DNA and seem to prefer binding to curved or bent DNA structures with high affinity.[10–13] HU may be involved in organizing negative supercoils in prokaryotic chromosomes into nucleosome-like structures, while its role in the overall packaging of bacterial DNA is obscure.[14] Furthermore, *in vitro* HU facilitates the formation of specific higher-order nucleoprotein complexes which regulate a variety of DNA transactions.[15–19]

Several studies have been performed to understand the interaction of HU with DNA at the molecular level. The structure of the 19.5 kDa HU protein from *Bacillus stearothermophilus* (HUBst), consisting of 90 amino acid residues per monomer, has been determined by x-ray crystallography,[20,21] and recently a high-resolution solution structure of the same protein has been determined using NMR data.[22] The structures of the core of HUBst are very similar with both techniques. The NMR data, however, revealed the nature of the extended flexible β-hairpin arms (residues 53–76) protruding from the hydrophobic core of the dimer into the solvent. The β-arms were proposed as the DNA-binding region of HUBst,[20] and their flexibility would facilitate binding in one of the DNA grooves. Biochemical and biophysical data obtained for several HU proteins indicate the involvement in DNA binding of some residues in the β-arms. By selective chemical modification of the hetero dimeric *E. coli* HU subunits, it was demonstrated that at least one arginine residue in the β-arms is necessary for DNA binding.[23] Further, photo-oxidation of His-54 resulted in the loss of the DNA-binding ability of *E. coli* HU.[23] The involvement of His-54 in DNA interaction was supported by NMR studies, which showed a significant change in chemical shift of the His-54 C-2 proton upon DNA binding.[24] Furthermore, from $^{13}C$ relaxation data on HUBst it was demonstrated that the mobility of the backbone at Gly-60 is significantly reduced by DNA binding.[25] Also for the homologous TF1 protein mutant (F61W), quenching of fluorescence of Trp-61 upon complexation with DNA demonstrates the involvement of the flexible arms in DNA interaction.[26]

Here we studied the interaction of HUBst with DNA by a variety of methods. First, we applied photochemically induced nuclear polarization (photo-CIDNP)[27] on a mutant of HUBst in which Met-69 in the tip and Val-76 in the stem of the β-hairpin arm are

* Author to whom correspondence should be addressed.

CCC 0749–1581/96/SI0081–06

*Received 1 July 1996*
*Accepted (revised) 7 October 1996*

replaced by tyrosines. For HUBst(M69Y; V76Y), a photo-CIDNP effect is observed for Tyr-69 in the tip of the $\beta$-hairpin arm, which is quenched upon DNA binding. Both these photo-CIDNP results and changes in chemical shifts indicate that the phenol ring of Tyr-69 is involved in DNA interactions. Finally, we studied the chemical shift perturbations and relaxation behavior of $^{15}$N-labeled wild-type HUBst protein. The effects observed on the $^{15}$N and $^{1}H^{N}$ chemical shifts of backbone and side-chain amide groups upon addition of DNA confirm the involvement of the $\beta$-hairpin arms of HUBst in DNA binding. In agreement with that, $^{15}N$–$^{1}H^{N}$ heteronuclear relaxation data reveal that for free HUBst the DNA-binding arms are highly mobile, whereas in DNA-complexed HUBst the arms are more rigid.

## EXPERIMENTAL

### Sample preparation

Cloning of the HUBst gene, overproduction and purification of the protein and the DNA-binding assay were described by Padas *et al.*[28] Using this recombination procedure native HUBst, a mutant HUBst(M69Y; V76Y) in which Met-69 and Val-76 were replaced by tyrosines, and $^{15}$N-labeled HUBst protein were prepared, the latter by using $^{15}NH_4Cl$ in a minimal medium. The proteins were purified employing affinity chromatography of heparin-Sepharose and Mono-S FPLC. The purity was >95% as judged by sodium dodecyl sulfate polyacrylamide gel electrophoresis (SDS-PAGE) and silver staining. Recombinant proteins were as active as the protein purified from *B. stearothermophilus* with respect to its DNA-binding properties. Oligomeric d(TCAAGGCCTTGA)$_2$ DNA, d(CAGACGTCTG)$_2$ DNA and d(CAGGCTTGCAAGCCTG)$_2$ DNA were used to form protein–DNA complexes with the mutant HUBst(M69Y; V76Y) and $^{15}$N-labeled HUBst, respectively.

### NMR spectroscopy

NMR experiments were performed with 1.0 mM protein samples at 311 K, containing 50 mM $KP_i$ buffer at pH 4.6 and 200 mM KCl. One- and two-dimensional (1D and 2D) NMR spectra were recorded on Bruker AMX500 and AMX/2 600 NMR spectrometers both equipped with three r.f. channels and a triple-resonance HCN probe with a shielded gradient coil and a 10 A gradient amplifier (Bruker BGU-10).

2D NOE[29,30] and TOCSY spectra[31] were acquired in a phase-sensitive mode using States-TPPI.[32] 2D NOE spectra were recorded with mixing times of 75 and 150 ms and TOCSY spectra were recorded with a MLEV-17 spin-lock of 70 ms. 2D NOE and TOCSY spectra were recorded, both in 95% $^{1}H_2O$–5% $^{2}H_2O$ and in $^{2}H_2O$, for native HUBst and for the free and the DNA-bound mutant HUBst(M69Y; V76Y) with 225 complex $t_1$ and 1024 complex $t_2$ increments with typical measuring times of 18 h. Spectral widths in both proton directions were 11.1 ppm, with the carrier positioned at 4.75 ppm. The $t_1$ and $t_2$ data were apodized with a $\pi/4$-shifted sine-bell function and the $t_1$ data were zero-filled to 1K points. Photo-CIDNP spectra were obtained as described in the legend of Fig. 1.

($^{15}$N, $^{1}$H)-HSQC experiments were recorded essentially as described by Bax *et al.*[33] $^{15}N$ $T_1$, $T_{1\rho}$ and heteronuclear $^{15}N$–$^{1}H^{N}$ NOE data sets were recorded as described essentially by Dayie and Wagner,[34] using for $T_{1\rho}$ experiments a spin-lock field of about 2.5 kHz. The HSQC, $T_1$, $T_{1\rho}$ and NOE pulse sequences were extended by a pulse scheme for sensitivity enhancement.[35,36] $^{15}N$–$^{1}H$ correlated data sets were acquired generally as 64 hypercomplex $t_1$ points and 512 complex $t_2$ points and processed into spectra of 512 × 2048 real data points. The spectral widths were 33.1 and 11.1 ppm in the $t_1$ and $t_2$ directions, respectively, with the $^{15}N$ and $^{1}H$ carrier frequencies at 119.1 and 4.75 ppm, respectively. Experiments were performed with protein samples in 95% $^{1}H_2O$–5% $^{2}H_2O$.

A series of ($^{15}$N, $^{1}$H)-HSQC experiments were recorded at 500 MHz, with 32 scans per $t_1$ increment, for $^{15}N$-labeled HUBst in the presence of increasing amounts of DNA. ($^{15}$N, $^{1}$H)-HSQC experiments were also recorded at 600 MHz for the initial and final sample, with 256 scans per $t_1$ increment. For both free and DNA-bound HUBst $^{15}N$ $T_1$, $T_{1\rho}$ and heteronuclear $^{15}N$–$^{1}H^{N}$ NOE experiments were recorded at 600 MHz with 48, 96 and 144 scans per $t_1$ increment, respectively. $^{15}N$ $T_1$ and $T_{1\rho}$ relaxation times were obtained by employing nine different relaxation delays ranging from 48 to 2000 and from 6 to 200 ms, respectively.

Both $T_1$ and $T_{1\rho}$ data sets were recorded and processed in such a way that the cross-peak volumes in the 2D spectra, as a function of the relaxation delay, would decay to zero. Relaxation times were obtained using the Levenburg–Marquardt algorithm for non-linear least-square minimization of the $\chi^2$-error function,[37] using as a model function a two-parameter monoexponential decay. Heteronuclear Overhauser enhancement factors, $\eta = (I_{sat} - I_0)/I_0$, were calculated from the normalized difference of the cross-peak volumes in the presence ($I_{sat}$) and absence ($I_0$) of $^{1}H$ saturation. All 2D spectra were processed using our NMR program package TRITON and analysed using the NMR analysis program ALISON on a Silicon Graphics Indy workstation.

## RESULTS AND DISCUSSION

### Interaction of mutant HUBst(M69Y; V76Y) with DNA

The interaction of HUBst(M69Y; V76Y) with 12 base pair DNA is characterized using the photo-CIDNP method, in which nuclear spin polarization is created through the interaction of a photo-excited dye with the substrate. Enhanced absorbtion or emission is observed for a number of amino acids (His, Tyr, Trp, Met) if they are accessible to the dye.[27,38] Figure 1(a) shows the aromatic 1D $^{1}H$ NMR spectrum of HUBst(M69Y; V76Y) recorded at 360 MHz. In the photo-CIDNP difference spectrum of free HUBst(M69Y; V76Y), as shown in Fig. 1(b), an enhanced emission signal is observed for the $H^{\varepsilon}$ protons of Tyr-69. However, no photo-CIDNP effect

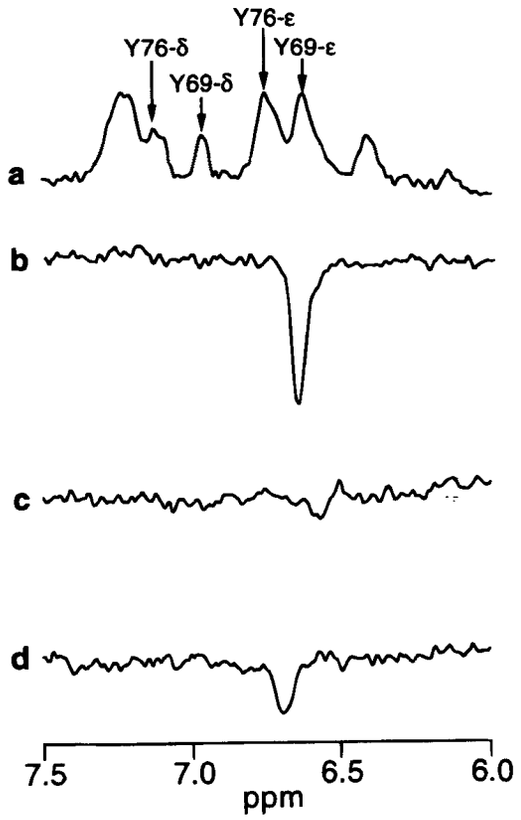


**Figure 1.** (a) Aromatic region of a one-dimensional $^1$H NMR spectrum of a 0.2 mM (dimer) solution of HUBst(M69Y; V76Y), pH 6.3 at 311 K, in $D_2O$ containing 50 mM phosphate, 200 mM KCl and 0.4 mM flavin I (dye). (b–d) Photo-CIDNP difference spectra of HUBst(M69Y; V76Y), (b) without DNA, (c) in the presence of 0.24 mM d(TCAAGGCCTTGA)$_2$ DNA and (d) with the same amount of DNA in 1.5 mM KCl. Photo-CIDNP spectra were recorded on a Bruker WM-360 spectrometer at 360 MHz as described previously,[27,38] using a light pulse of 0.5 s and 4 W laser power. A line broadening of 4 Hz was applied for all spectra. Chemical shifts are refered to a flavin signal at 7.98 ppm.

was observed for the H$^\varepsilon$ protons of Tyr-76, indicating that the OH group of Tyr-76 is not accessible to the dye in the free protein and may be involved in an intramolecular hydrogen bond. Figure 1(c) and (d) show that in the presence of DNA with respect to the protein the enhanced signal of the H$^\varepsilon$ protons of Tyr-69 is quenched, but that it is partially recovered after addition of 1.5 M KCl. The quenching of the photo-CIDNP effect in the presence of DNA indicates that Tyr-69 is involved in DNA binding and not accessible for the flavin dye in the protein–DNA complex. At high salt concentrations electrostatic interactions between protein and DNA are reduced, which resulted in partial release of the protein from the oligonucleotide.

Previously, complete $^{15}$N, $^{13}$C and $^1$H assignments have been reported for wild-type HUBst.[40] The two aromatic tyrosine H$^\delta$ and H$^\varepsilon$ proton resonances of the mutant HUBst(M69Y; V76Y) were easily identified from the $^1$H NMR spectrum and from the 2D NOE and TOCSY spectra. Although some of the $^1$H chemical shifts of residues near the tyrosines have changed, most of the chemical shifts and NOE connectivities are the same for HUBst(M69Y; V76Y) and for native HUBst. This implies that the tertiary folding of the dimeric protein HUBst is not influenced by mutagenesis of two tyrosine residues at positions 69 and 76 in the $\beta$-arm region of each monomer of the protein.

The mutant HUBst(M69Y; V76Y) was titrated with a 12 base pair DNA fragment. Figure 2 shows how the aromatic $^1$H NMR spectrum of the HUBst mutant is affected by the addition of DNA. Chemical shifts of both H$^\delta$ and H$^\varepsilon$ protons of Tyr-69 move upfield by 0.1 ppm, whereas the aromatic $^1$H chemical shifts of Tyr-76 and of the four phenylalanine amino acid residues are not changed upon addition of DNA. The changes in the aromatic $^1$H chemical shifts of Tyr-69 support our results of the photo-CIDNP experiment described above. Furthermore, a comparison of 2D NOE spectra of the free and DNA-bound HUBst(M69Y; V76Y) reveals that most NOE connectivities are preserved, indicating that no substantial changes in the conformation of the core of the protein occur upon binding to DNA. Unfortunately, no protein–DNA NOEs could be observed, possibly due to the non-specific binding character of HUBst.

### Titration of $^{15}$N-labeled HUBst with double-stranded DNA

$^{15}$N-labeled HUBst was titrated both with 10 and 16 base pair (bp) DNA fragments, the latter containing one

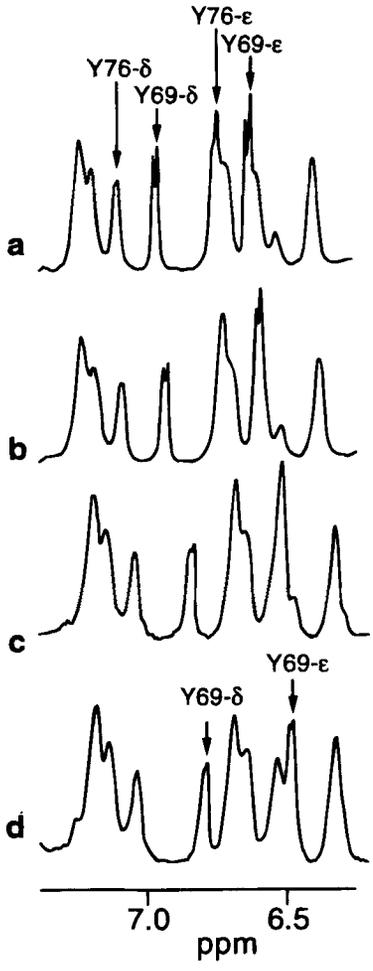


**Figure 2.** Aromatic region of the 500 MHz $^1$H NMR spectrum of the mutant HUBst(M69Y; V76Y) at different molar DNA to protein ratios: (a) 0%, (b) 30%, (c) 60% and (d) 100%. In this experiment DNA was added to the protein.

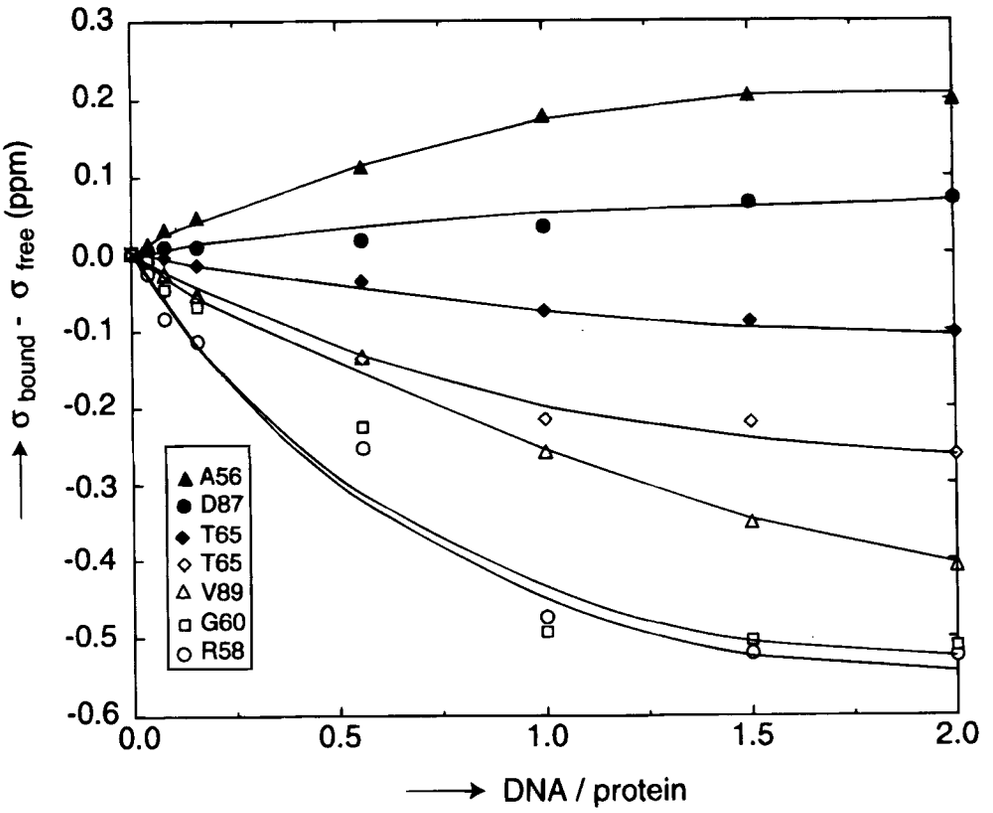


**Figure 3.** *Titration curves* of some backbone $^{15}N$ and $^{1}H^{N}$ chemical shifts of HUBst upon adding d(CAGACGTCTG)$_2$ DNA. Chemical shifts were obtained from ($^{15}N$, $^{1}H$)-HSQC spectra recorded at 500 MHz. The differences in the chemical shifts are displayed relative to the chemical shift for the protein without DNA ($\sigma_{free}$). Open and filled data points correspond to $^{15}N$ and $^{1}H^{N}$ chemical shifts, respectively.

of the prefered binding sequences of HU in bacteriophage Mu DNA, as characterized by nuclease cleavage data.[41] Figure 3 shows the titration curves of some $^{15}N$ and $^{1}H^{N}$ chemical shifts, for which large shifts were measured from ($^{15}N$, $^{1}H$)-HSQC spectra in the presence of increasing amounts of the 10 bp DNA fragment. Similar results were obtained for the 16 bp fragment (data not shown). The curves have all reached a stationary value in the situation where all DNA was added, which demonstrates that virtually all of the protein is bound to DNA.

Figure 4(A) and (B) show the backbone $^{15}N$ and $^{1}H^{N}$ chemical shift differences between bound and free HUBst, respectively, as a function of the residue number. Large backbone $^{15}N$ shifts (>0.2 ppm) and $^{1}H^{N}$ shifts (>0.05 ppm) are observed for many residues present in the β-hairpin arm of HUBst, such as Glu-54, Ala-56, Arg-58, Lys-59, Gly-60, Asn-62, Thr-65, Met-69 and Val-76. Significant changes in the $^{15}N$ and $^{1}H^{N}$ chemical shifts are also observed for residues in the three-stranded anti-parallel β-sheet, located at the same site of HUBst as the two β-hairpin arms, such as Asp-40, Val-42, Leu-44, Ile-45, Gly-46 and Phe-79. These results again demonstrate the involvement of the β-arms in DNA interaction. Additionally, large changes of $^{15}N$ and/or $^{1}H^{N}$ chemical shifts are observed for Asp-87, Val-89 and Lys-90, indicating that, besides the β-arm region, also the second half of the third α-helix of HUBst may be involved in DNA binding. Likewise, the *C*-terminal amino acids of the related IHF α- and β-subunits and of the homodimer TF1 were also proposed to interact with DNA.[42–44] The changes in the side-chain $^{15}N$ and $^{1}H^{N}$ chemical shifts of HUBst in the presence of DNA are presented in Table 1. Large chemical shift differences were observed for $N^{\delta}$ of Asn-62, for $N^{\varepsilon}$ of Arg-37 and Arg-55 and for $H^{\varepsilon}$ of Arg-37, Arg-55, Arg-58 and Arg-61. Except for Arg-37, these residues are all present in the β-arm region of

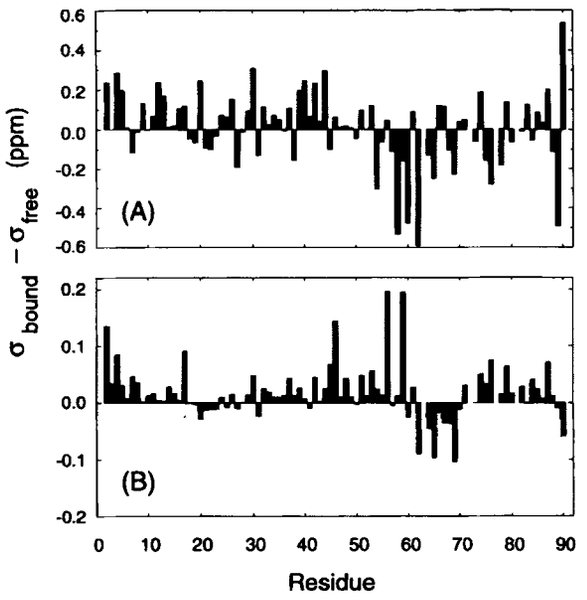


**Figure 4.** Differences between (A) backbone $^{15}N$ and (B) backbone $^{1}H^{N}$ chemical shifts of HUBst bound to d(CAGACGTCTG)$_2$ DNA ($\sigma_{bound}$) and free in solution ($\sigma_{free}$) as a function of the amino acid residue number. Chemical shifts (in ppm) were measured from ($^{15}N$, $^{1}H$)-HSQC spectra recorded at 600 MHz.

**Table 1. Differences between side-chain $^{15}N$ and $^{1}H^{N}$ chemical shifts of HUBst bound to d(CAGACGTCTG)$_2$ DNA and free in solution**

| Residue | $\sigma_{bound}-\sigma_{free}$* (ppm) $^{15}N^{\delta}/^{15}N^{\varepsilon}$ | $^{1}H^{\delta1}/^{1}H^{\varepsilon1}$ | $^{1}H^{\delta2}/^{1}H^{\varepsilon2}$ |
|---|---|---|---|
| Asn-2 | 0.10 | 0.05 | −0.01 |
| Asn-8 | 0.02 | 0.01 | 0.02 |
| Arg-37 | −0.17 | 0.11 | — |
| Gln-43 | −0.07 | 0.05 | 0.02 |
| Asn-49 | −0.07 | 0.05 | 0.02 |
| Arg-53 | 0.10 | 0.03 | — |
| Arg-55 | −0.29 | 0.10 | — |
| Arg-58 | 0.04 | 0.10 | — |
| Arg-61 | −0.04 | 0.14 | — |
| Asn-62 | −0.19 | 0.01 | −0.05 |
| Gln-64 | −0.04 | −0.03 | −0.03 |

*Chemical shifts were measured from ($^{15}N$, $^{1}H$)-HSQC spectra recorded at 600 MHz.

HUBst. Less significant are the changes of one of the side-chain $NH_2$ protons of Asn-2, Gln-43, Asn-49 and Asn-62.

### Analysis of heteronuclear NOEs and of $T_1$ and $T_{1\rho}$ relaxation times

The proposed DNA-binding model for HUBst, in which the highly flexible $\beta$-hairpin arms wrap around the DNA, suggests that the mobility of this DNA-binding region reduces in the protein–DNA complex. A very sensitive probe for the internal dynamics of the amide nitrogen–proton vectors is the $^{15}N$–$^{1}H^{N}$ heteronuclear NOE.[45] Figure 5(A) and (B) show plots of the backbone $^{15}N$–$^{1}H^{N}$ heteronuclear NOE at a $^{15}N$ frequency of 60.9 MHz as a function of the amino acid sequence of HUBst free in solution and bound to DNA, respectively. For free HUBst the values of $\eta$ close to $-1$, associated with several residues in the tip of the $\beta$-arms, indicate that the $\beta$-arms are highly flexible. In the protein–DNA complex, the value $\eta$ increases significantly for the residues in the $\beta$-arms, indicating that the mobility is reduced upon binding. However, we note that the high-frequency flexibility, as represented by the heteronuclear NOE, partly remains. This cannot be due to incomplete binding, since the binding experiments indicate that most of HU was bound to the DNA (see above). Apparently, flexibility of the DNA-binding arms of HU is still present in the complex. Similar observations have been made in a complex of *lac* repressor headpiece (1–56) with DNA.[46]

Another probe for the dynamics of the protein backbone is the $^{15}N$ $T_{1\rho}$ relaxation time, which is more sensitive to lower frequency motions of the N—H bonds. Figure 6(A) and (B) show the backbone $^{15}N$ $T_{1\rho}$ values of HUBst as a function of the amino acid sequence for the protein free in solution and in the protein–DNA complex. In the complex the $T_{1\rho}$ values for the residues in the tip of the $\beta$-hairpin arm have changed substantially with respect to the free protein to values that are only slightly higher than those observed for residues in the core of the protein. These changes are consistent with those observed for the heteronuclear NOE and confirm that the mobility of the $\beta$-arms of HUBst

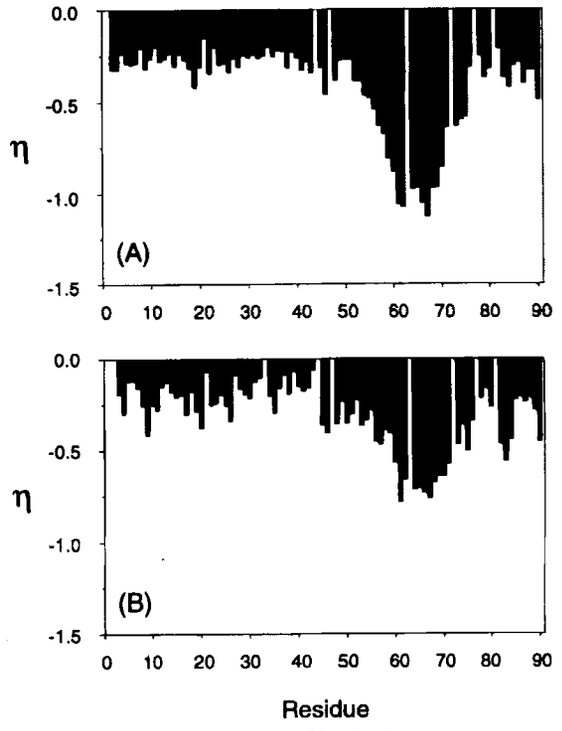


**Figure 5.** Backbone heteronuclear $^{15}N$–$^{1}H^{N}$ NOE as a function of the amino acid residue number for HUBst (A) free in solution and (B) bound to DNA. The enhancement factor $\eta$ was calculated as $(I_{sat}-I_0)/I_0$, where $I_{sat}$ and $I_0$ are the cross-peak volumes in the presence and absence of proton saturation, respectively. Cross-peak volumes were extracted from spectra recorded at 600 MHz.

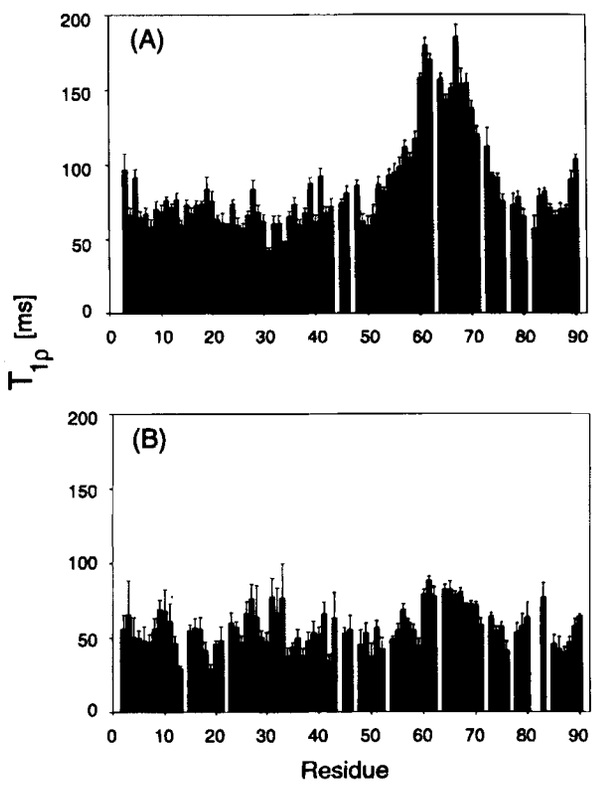


**Figure 6.** Bar graphs of the backbone $^{15}N$ $T_{1\rho}$ relaxation time as a function of the amino acid sequence for HUBst (A) free in solution and (B) bound to DNA, measured at 600 MHz and 38 °C. Blank slots indicate prolines or severely overlapped residues.

reduces when the protein binds to DNA. $^{15}N$ $T_1$ relaxation times were measured likewise for the backbone of HUBst in its free and bound form. For residues 60–69 in the tip of the β-arms the average $T_1$ relaxation time changes from 743 ms for free protein to 899 ms for protein in the complex, which also indicates a reduction of the mobility of these arms. For the residues in the hydrophobic core of the protein dimer the average $^{15}N$ $T_1$ value changes from 819 ms for the free protein to 1272 ms in the protein–DNA complex. The average $^{15}N$ $T_{1\rho}$ value changes from 70 to 53 ms in the complex. This corresponds to an increase of the overall rotational correlation time from $10.6 \pm 0.9$ ns for the free protein to $15.6 \pm 2.2$ ns for the protein–DNA complex, under the assumption that for these residues the effect of internal motions can be neglected.[45] A quantitative analysis of the mobility of the backbone of HUBst using relaxation data at different magnetic field strengths is currently in progress.

In summary, a variety of NMR experiments have indicated quenching of surface accessibility for the solvent, changes of the electronic environment and of the dynamics of the β-hairpin arm region and of parts of the three-stranded anti-parallel β-sheet region of HUBst when it binds to DNA. Additionally, evidence was found that the few last residues of the protein located in the third α-helix may be important for binding to DNA. These results confirm the previously proposed DNA-binding model for HU in which the DNA binds into the β-sheet region after which the flexible arms wrap around the DNA. While the longer *C*-terminal α-helices in IHF and TF1 had been implicated to be involved in DNA binding, this had not been noted for HU proteins, where this α-helix is considerably shorter. A model-building study (unpublished results) suggests that simultaneous binding of the β-ribbon arms and the *C*-terminal α-helices of the HU dimer is only possible when DNA is bent.

## Acknowledgements

This work was supported in part by the Netherlands Foundation for Chemical Research (SON) with financial support from the Netherlands Organization for Scientific Research (NWO). The authors thank Dr P. Pouwels for assisting with setting up the photo-CIDNP experiments.

## REFERENCES

1. K. Drlica and J. Rouviere-Yaniv, *Microbiol. Rev.* **51**, 301 (1987).
2. D. E. Pettijohn, *J. Biol. Chem.* **263**, 12793 (1988).
3. D. I. Friedman, *Cell* **55**, 545 (1988).
4. S. Goodman, C. Yang, H. A. Nash, A. Sarai and R. Jernigan, *Structure and Methods 2*, pp. 51–62. Adenine Press Schenectady, NY, USA (1990).
5. C. C. Yang and H. A. Nash, *Cell* **57**, 869 (1989).
6. C. C. Yang and H. A. Nash, *Proc. Natl. Acad. Sci.* **91**, 12183 (1994).
7. J. R. Green and E. P. Geiduschek, *EMBO J.* **4**, 1345 (1985).
8. E. P. Geiduschek, G. J. Schneider and M. H. Sayre, *J. Struct. Biol.* **104**, 84 (1990).
9. A. M. Segall, S. D. Goodman and H. A. Nash, *EMBO J.* **13**, 4536 (1994).
10. H. A. Nash, *Trends Biochem. Sci.* **15**, 222 (1990).
11. R. E. Harrington, *Mol. Microbiol.* **6**, 2549 (1992).
12. A. Pontiggia, A. Negri, M. Beltrame and E. Bianchi, *Mol. Microbiol.* **7**, 343 (1993).
13. M. Serrano, M. Salas and J. M. Hermosa, *Trends Biochem. Sci.* **18**, 202 (1993).
14. M. B. Schmid, *Cell* **63**, 451 (1990).
15. R. Johnson, M. Bruist and M. Simon, *Cell* **46**, 531 (1986).
16. B. Funnel, T. Baker and A. Kornberg, *J. Biol. Chem.* **262**, 10327 (1987).
17. Y. Flashner and J. D. Gralla, *Cell* **54**, 713 (1988).
18. H. Echols, *J. Biol. Chem.* **265**, 14697 (1990).
19. M. G. Surette and G. Chaconas, *Cell* **68**, 1101 (1992).
20. I. Tanaka, K. Appelt, J. Dijk, S. W. White and K. S. Wilson, *Nature (London)* **310**, 376 (1984).
21. S. W. White, K. Appelt, K. S. Wilson and I. Tanaka, *Proteins* **5**, 281 (1989).
22. H. Vis, M. Mariani, C. E. Vorgias, K. S. Wilson, R. Kaptein and R. Boelens, *J. Mol. Biol.* **254**, 692 (1995).
23. M. Lammi, M. Paci and C. B. Gualerzi, *FEBS Lett.* **170**, 99 (1984).
24. H. Shindo, H. Kurumizaka, A. Furubayashi, C. Sakuma, U. Matsumoto, A. Yanagida, N. Goshima, Y. Kano and F. Imamoto, *Biol. Pharm. Bull.* **16**, 437 (1993).
25. Y. Kakuta, H. Hojo, S. Aimoto, I. Tanaka and K. Hikichi, *J. Biochem.* **116**, 1153 (1994).
26. T. Härd, M. H. Sayre, E. P. Geiduschek and D. R. Kearns, *Biochemistry* **28**, 2813 (1989).
27. R. Kaptein, in *Biological Magnetic Resonance*, Vol. 4, edited by L. J. Berliner and J. Reuben, pp. 145–219. Plenum Press, New York (1982).
28. P. M. Padas, K. S. Wilson and C. E. Vorgias, *Gene* **117**, 39 (1992).
29. J. Jeener, B. H. Meier, P. Bachmann and R. Ernst, *J. Chem. Phys.* **71**, 4546 (1982).
30. D. J. States, R. A. Haberkorn and D. J. Ruben, *J. Magn. Reson.* **48**, 286 (1982).
31. A. Bax and D. G. Davis, *J. Magn. Reson.* **65**, 355 (1985).
32. D. Marion, M. Ikura, R. Tschudin and A. Bax, *J. Magn. Reson.* **85**, 393 (1989).
33. A. Bax, M. Ikura, L. E. Kay, D. A. Torchia and R. Tschudin, *J. Magn. Reson.* **86**, 304 (1990).
34. K. T. Dayie and G. Wagner, *J. Magn. Reson.* **A111**, 121 (1994).
35. J. Cavanagh, A. G. Palmer III, P. E. Wright and M. Rance, *J. Magn. Reson.* **91**, 429 (1991).
36. L. E. Kay, P. Keifer and T. Saarinen, *J. Am. Chem. Soc.* **114**, 10663 (1992).
37. W. H. Press, S. A. Teukolsky, W. T. Vettering and B. P. Flannery, *Numerical Recipes*. Cambridge University Press, Cambridge (1992).
38. S. Stob and R. Kaptein, *Photochem. Photobiol.* **49**, 565 (1989).
39. S. Stob, R. M. Scheek, R. Boelens and R. Kaptein, *FEBS Lett.* **239**, 99 (1988).
40. H. Vis, R. Boelens, M. Mariani, R. Stroop, C. E. Vorgias, K. S. Wilson and R. Kaptein, *Biochemistry* **33**, 14858 (1994).
41. B. D. Lavoie and G. Chaconas, *Genes Dev.* **7**, 2510 (1993).
42. M. H. Sayre and E. P. Geiduschek, *J. Virol.* **62**, 3455 (1988).
43. A. E. Granston and H. A. Nash, *J. Mol. Biol.* **234**, 45 (1993).
44. G. Mengeritsky, D. Goldenberg, I. Mendelson, H. Giladi and A. B. Oppenheim, *J. Mol. Biol.* **231**, 646 (1993).
45. L. E. Kay, D. A. Torchia and A. Bax, *Biochemistry* **28**, 8972 (1989).
46. M. Slijper, PhD Thesis, University of Utrecht (1996).